*Journal of the European Ceramic Society* **6** (1990) 89–95

# Fatigue of Silicon Nitride Ceramics under Cyclic Loading*

S. Horibe

National Research Institute for Metals, Tsukuba Laboratories, Sengen, Tsukuba-City, Ibaraki 305, Japan

(Received 16 October 1989; revised version received 29 January 1990; accepted 31 January 1990)

***Abstract***

*Cyclic fatigue behavior of normally sintered and reaction-bonded silicon nitride materials was investigated from the microstructural point of view. It has been found that in any silicon nitride material the crack propagates by cyclic loading even under the condition of* $K_{max} < K_{ISCC}$, *and that surface upheavals (microscopic lifting of the surface) and different type of cracks are produced in the region near the cyclically propagating cracks. It is supposed that asperity-contacts of crack surfaces are closely related to the fatigue damage behavior.*

*Das zyklische Ermüdungsverhalten von normal gesinterten und reaktionsgebundenen* $Si_3N_4$*-Werkstoffen wurde hinsichtlich des Gefügeeinflusses untersucht. Es wurde beobachtet, daß in allen* $Si_3N_4$*-Werkstoffen der Riß unter Dauerschwingbeanspruchung sogar schon bei* $K_{max} < K_{ISCC}$ *fortschreitet, und daß Oberflächenverwerfungen und verschiedene Rißtypen in der Nähe des zyklisch fortschreitenden Risses auftreten. Es wird angenommen, daß die Riß flankenwechselwirkung der Rißoberfläche eng mit dem Ermüdungsschaden verknüpft ist.*

*On a étudié le comportement en fatigue cyclique de matériaux à base de nitrure de silicium densifiés par frittage classique ou par frittage réactif, du point de vue de la microstructure. Dans tous les matériaux étudiés, la fracture se propage même dans le cas où* $K_{max} < K_{ISCC}$ *et des soulèvements de la surface ainsi que différentes sortes de craquelures sont produites à la proximité des fissures se propageant par contrainte cyclique. On suppose que les contacts aspérité-fissure sont en relation étroite avec le comportement en fatigue.*

*Paper presented at the Advanced Materials Science and Engineering Society Conference '89, Tokyo, 16–17 March 1989 (co-chairmen Y. Matsuo and M. Sakai).

## 1 Introduction

The fatigue of ceramic materials under cyclic loading has recently started to be regarded as an important problem, because of the demand for high-performance structural ceramic materials. The amount of fatigue data is increasing, but the mechanism by which fatigue cracking occurs remains unexplained. In metals and alloys, fatigue damage is attributed to irreversible plastic deformation caused by dislocation motion. This process is not considered to be the dominant one in ceramic materials. Although some alternative models or mechanisms have been proposed,[1–6] experimental evidence is lacking.

It is the main aim of this paper to obtain fundamental knowledge, focusing on the silicon nitride ceramics from the microstructural point of view, which would be helpful in determining possible fatigue mechanisms.

## 2 Experimental Procedure

### 2.1 Materials

The silicon nitride materials studied are shown in Table 1. Material A was normally sintered with $Y_2O_3$–$MgAl_2O_4$ additives, whereas Materials B, C and D were reaction-bonded. Material B was processed at 1450°C and consisted of a mixture of $\alpha$- and $\beta$-phase crystals. Material C was obtained from Material B by post-heating at 1700°C (for 5 h) to transform the $\alpha$ phase to the $\beta$ phase. As well as the different phase content of Materials B and C, there is another difference in microstructures, that is in micropore size. Micropore size is considered to have



*Journal of the European Ceramic Society* 0955-2219/90/$3.50 

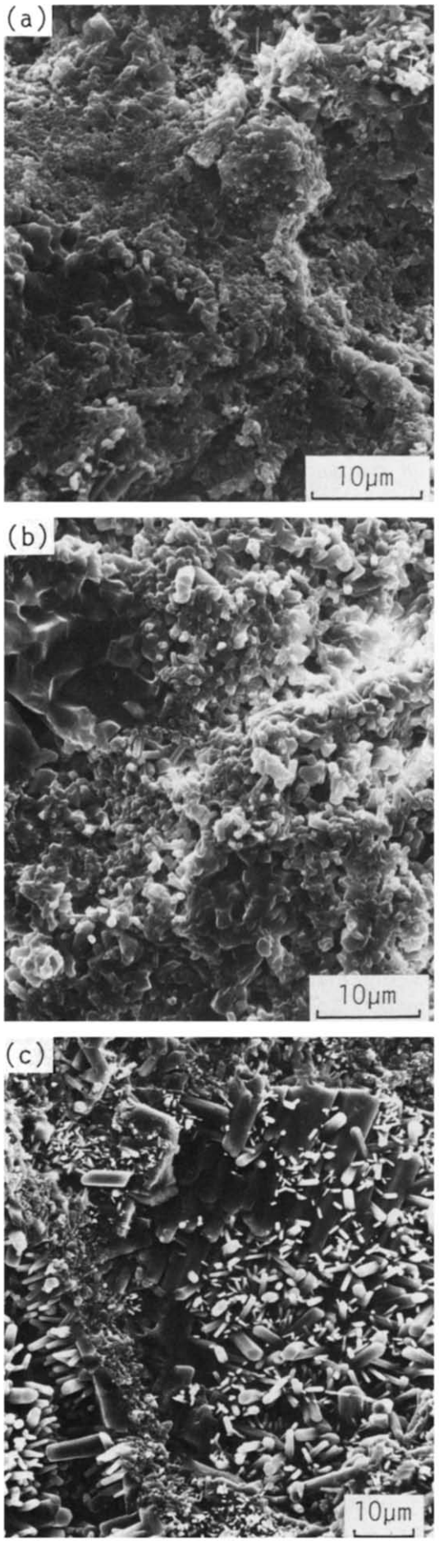


a greater effect than phase on the mechanical properties of a material.[7,8] Material D was made from a different silicon powder of the higher purity. It was processed at 1500°C and is entirely $\beta$ phase. The pore volume fraction of the sintered Material A is <2%, whereas those of the reaction-bonded materials are extremely high: ~15% in Materials B and C, and ~34% in Material D. Figure 1 shows scanning electron micrographs of the fracture surfaces of Materials B, C and D, which indicate the differences in shapes and sizes of the particles of the three materials.

These materials, with dimensions of about 4 mm × 5 mm × 45 mm, were ground and lapping-polished to produce the specimens for fatigue test, with dimensions of 3 mm × 4 mm × 40 mm. Before fatigue testing, one or three precracks were introduced at the center of the specimen by a Vickers indentor, using a load of 98 N. Fatigue tests using the specimens with three precracks provide conservative data for the fatigue lives of materials, compared with the tests of the specimens with a single crack.

### 2.2 Fatigue test

Fatigue tests were conducted in four-point bending (outer span 30 mm, inner span 10 mm) at a frequency of 3 or 20 Hz, using an electrohydraulic testing system. All experiments were carried out at room temperature in air. In this study, two types of test procedures have been adopted, for different purposes.

#### *2.2.1 Fatigue Test A*

This test was to judge the effect of cyclic loading. Test A is considered to be the simplest and most reliable method to check whether or not there exists a cyclic loading effect in the material.[9,10] First, the specimens are statically loaded for a sufficient period of time at the maximum stress of the loading cycle for the complete arrest of crack propagation. They are then cyclically loaded and the crack growth behavior during this period is observed. The crack length was measured by an optical microscope, at magnification ×400, by interrupting the testing and taking the specimen off the machine. The accuracy of this crack length measurement was about $\pm 2 \times 10^{-3}$ mm. This provides information on the crack growth during cyclic loading below $K_{ISCC}$ (the lowest stress intensity factor for stress corrosion cracking to occur); in other words, at values of $K_{max}$ (the

**Fig. 1.** Scanning electron micrographs of the fracture surfaces of the three reaction-bonded silicon nitride ceramics: (a) Material B; (b) Material C; (c) Material D.

**Table 1.** Processing conditions and characteristics of materials used

| | *Processing method* | *Processing conditions* | *Phase* | *Density* ($g/cm^3$) | *Micropore size* |
|---|---|---|---|---|---|
| Material A | Sintered | Additives: $Y_2O_3$–$MgAl_2O_4$ Temperature: 1750°C | $\beta$ | 3·2 | — |
| Material B | Reaction-bonded | Temperature: 1450°C | $\alpha+\beta$ | 2·69 | Small |
| Material C | Reaction-bonded | Post-heating of Material B at 1700°C | $\beta$ | 2·69 | Large |
| Material D | Reaction-bonded | Temperature: 1500°C | $\beta$ | 2·10 | Large |

maximum stress intensity factor during cyclic loading) lower than those required for static fatigue. The rationale of this test procedure is easily understandable from the configuration of the stress intensity factor $K$, which consists of the residual stress component $K_r$ and the external stress component $K_a$ in the material with an indentation-induced crack,[11] as illustrated in Fig. 2. The details have been described elsewhere.[9,10]

*2.2.2 Fatigue Test B*

This test was for $S$–$N$ curve determination. In Test B the indented specimens are cyclically loaded without preliminary static loading and the fatigue lives are measured for various applied stress levels. As there exist residual tensile stresses at the crack tips caused by the Vickers indentation, the fatigue lives measured might be a little shorter than that of a specimen with a natural crack of the same size. However, this seems to cause no problem for a relative comparison of the $S$–$N$ curves of the materials used.

## 3 Experimental Results

### 3.1 Fatigue properties

Figure 3 shows the fatigue crack growth behavior obtained by using Test A. In every material, crack growth and its subsequent arrest was seen during static loading. It has been observed that a subsequent cyclic loading makes the crack propagate again. This result indicates that a cyclic loading effect exists even for the condition of $K_{max} < K_{ISCC}$ in all the silicon nitride ceramics, irrespective of the material fabrication method or its resultant microstructure.

Figure 4 shows the $S$–$N$ curves for the four materials. To obtain the same unloading condition in each test, the minimum stress during the cyclic process was kept nearly constant at ~9·8 MPa. It seems that each curve is composed of three regions (I, II and III), as illustrated schematically in Fig. 5. It is usual for $S$–$N$ curves to have only two regions (II and III). In region II the fatigue life depends on the stress amplitude, whereas in region III a fatigue limit is provided, below which the material never fails.

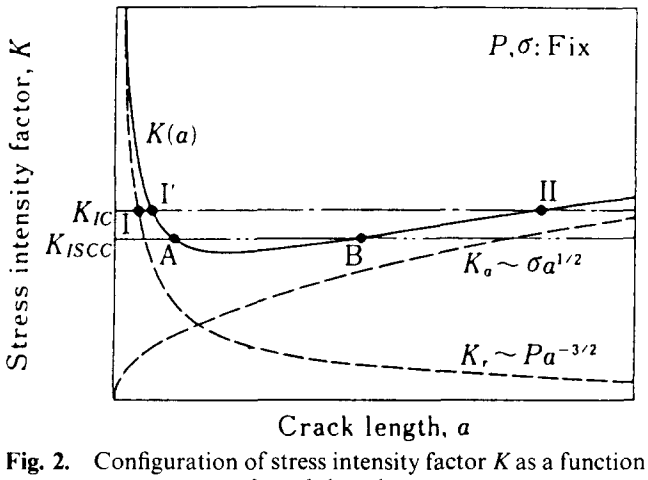


**Fig. 2.** Configuration of stress intensity factor $K$ as a function of crack length $a$.

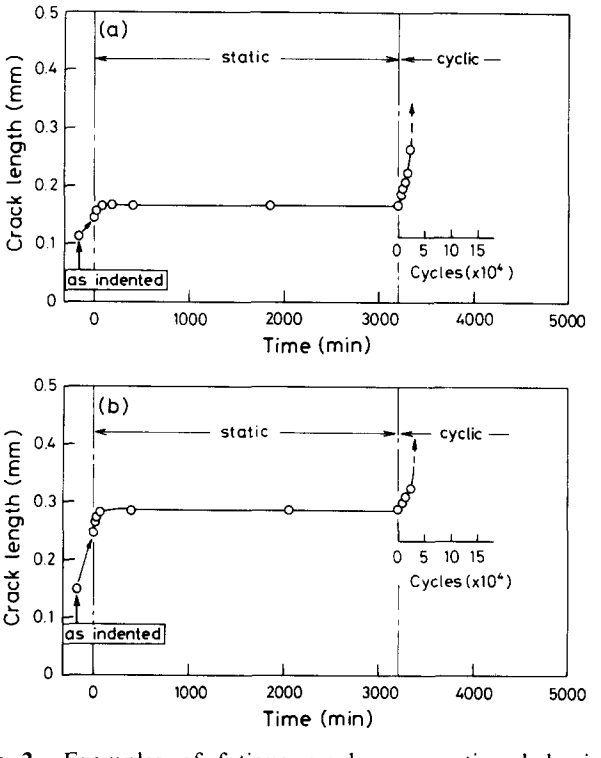


**Fig. 3.** Examples of fatigue crack propagation behavior obtained by using Test A ($R=0{\cdot}3$, $f=3$ Hz): (a) Material A, $\sigma_{max}=270$ MPa; (b) Material B, $\sigma_{max}=104$ MPa. Similar behavior was observed also in Materials C and D.

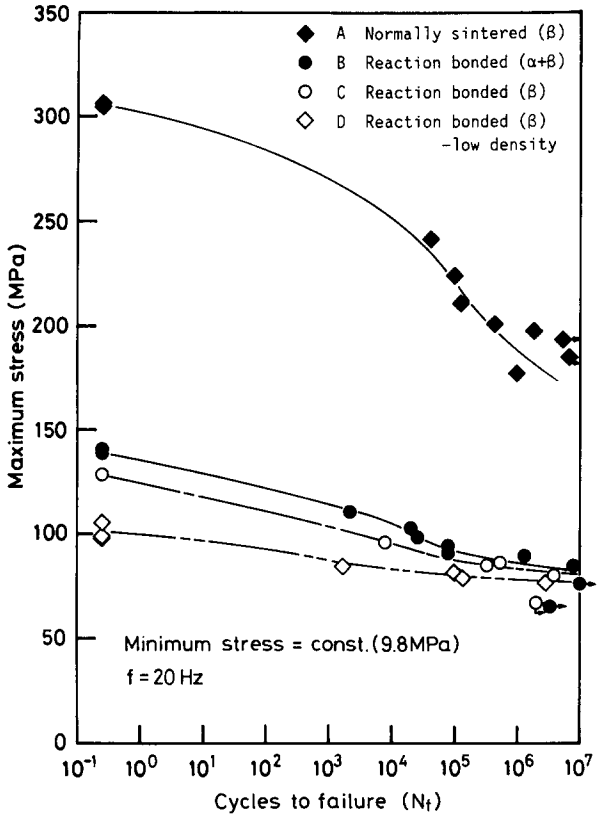


**Fig. 4.** *S–N* curves for the four silicon nitride materials.

Region I is observed in some metallic materials when the material damage is affected by time-dependent factors such as creep or stress corrosion cracking (SCC). The presence of region I in the curves of the present materials implies that static fatigue due to SCC is superimposed on the cyclic fatigue at relatively high stress amplitudes.

It should be noted that in the three reaction-bonded materials there are distinct differences of the flexural strength or the fatigue strength at a relatively low-cycle (high-stress) region, depending on the volume fraction and the pore size. It is of interest, however, that there are insignificant differences in their fatigue limits. As the fatigue limit in precracked material corresponds to the threshold value for crack propagation, the above result

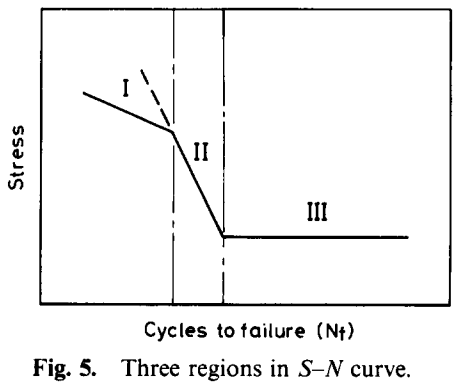


**Fig. 5.** Three regions in *S–N* curve.

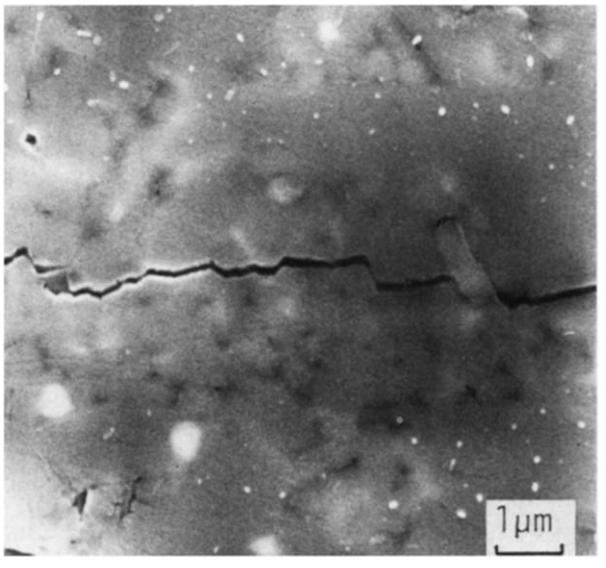


**Fig. 6.** Conventional scanning electron micrograph of a surface crack in Material A that has been cyclically fatigued.

indicates that the threshold condition might be determined by the unique value characteristic of the reaction-bonded $Si_3N_4$ materials, independently of microstructures such as the pore density and pore sizes.

### 3.2 Morphology of surface crack areas

Figure 6 shows a conventional scanning electron micrograph of a surface fatigue crack in Material A. It has been seen that cracks propagate intergranularly; however, the details in morphology of the near-crack area are not clear. Therefore, an electron surface analyser (ESA-3000, Elionix Inc.), in which surface topography information can be obtained by adopting two sets of secondary electron detectors, was used. The difference signals of secondary electrons provide information on the surface morphology, and it has been found that a surface upheaval (a raising of the surface) is produced in the near-crack region (Fig. 7(a)). Quantitative analyses have revealed that the width of the upheaval is $\sim 0{\cdot}1\ \mu m$ and its height is $\sim 0{\cdot}02\ \mu m$ (Fig. 7(b)). The original surface roughness was $< 0{\cdot}01\ \mu m$ and smoother than the upheaval so that such upheavals can be easily distinguished. A similar morphology has also been observed in the reaction-bonded materials. It is assumed that these upheavals are the plastic zones due to the asperity-contact of the crack surfaces.

The specimen shown in Fig. 7 was retested by the fatigue machine and the same area was observed by the electron surface analyser. The resulting surface morphology is shown in Fig. 8. It should be noted that the main crack tends to propagate in a different

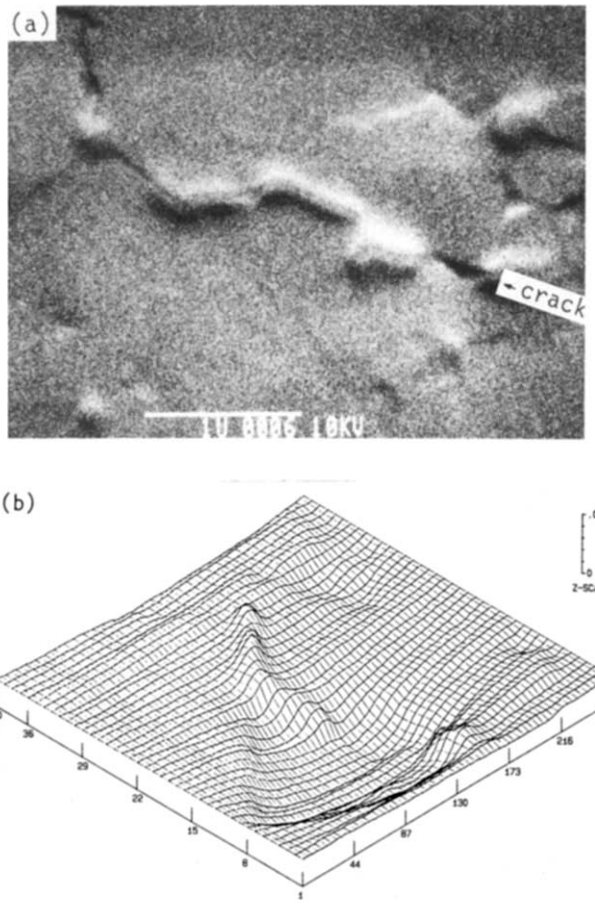


**Fig. 7.** The surface morphology of Material A provided by the difference signals of secondary electrons: (a) topographic scanning electron micrograph; (b) an example of quantitative analysis data.

path, which is sited at the base of a hill. The observation of such crack behavior implies the operation of a fatigue mechanism peculiar to ceramic materials. Details are discussed in the next section.

### 3.3 Macroscopic aspects of fracture

When the material is monotonically, statically or cyclically loaded, the precrack introduced by the Vickers indentor with relatively high load tends to grow to the final failure, as can be seen in Materials A, B and C. However, when Material D is monotonically loaded, the crack growth occurred not at the introduced flaw but at a different site (Fig. 9(a)). This means that some of the pre-existing flaws in the material are larger than those introduced by the indentation. This seems reasonable, as Material D has an extremely low density. In spite of this, it has been unexpectedly observed that during cyclic loading cracks introduced by the indentation propagate through the specimen, which is finally divided into two pieces (Fig. 9(b)). This suggests that the indentation should produce the states or

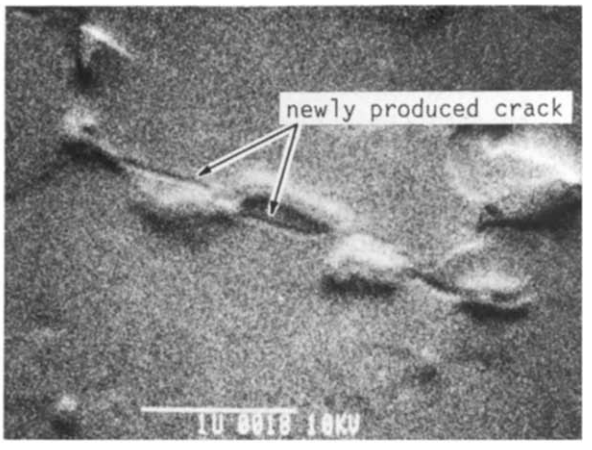


**Fig. 8.** Topographic scanning electron micrograph taken after the specimen shown in Fig. 7(a) was retested.

conditions suitable for the accumulation of cyclic damage, i.e. an indentation-induced crack must have different characteristics from the originally existing flaws, and it is more susceptible to cyclic fatigue damage despite its short length.

## 4 Discussion

Although the basic mechanisms for cyclic fatigue of ceramic materials have not yet been clarified, some possible mechanisms can be proposed.[2-6] Unfortunately, at present any mechanism cannot be strongly supported, because of the lack of conclusive data.

For cyclic crack propagation to occur, one of the following two conditions must be realized at the crack tip:

(1) An actual $K$ value higher than $K_{ap}$ (the apparent maximum stress intensity factor) is produced at the crack tip during cyclic loading. If this $K$ exceeds $K_{ISCC}$ for some reason, the crack might propagate during cyclic loading even for the condition of $K_{ap} <$

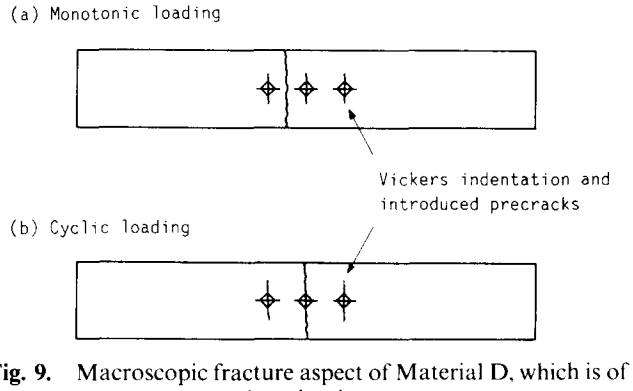


**Fig. 9.** Macroscopic fracture aspect of Material D, which is of low density.

$K_{ISCC}$. This is nothing but the accumulation of static fatigue damage.

(2) An irreversible new state of microstructure, in which the solid fails more easily, is created at the crack or the crack tip during cyclic loading. In this case, it is not necessary that $K$ exceeds $K_{ap}$.

The mechanisms proposed so far which appear to satisfy either one or both of these conditions are briefly summarized as follows.

### 4.1 Irreversible plastic deformation due to dislocation motion

This is a basic process for the fatigue of metals and alloys, and might be plausible also for the fatigue of some ceramic materials at high temperatures where the dislocation motion is active. However, it is not considered to be the dominant process for room-temperature fatigue of polycrystalline ceramic materials.

### 4.2 Residual stresses

In ceramic materials there are significant residual stresses which result from thermal contraction anisotropy.[2-4] Lewis[5] considered that the fatigue damage effects may take place through a change in fracture mode during test cycle; for example, from Mode I during the tension part to Modes II or III during the compression part. Lewis and Rice[4] proposed another type of mechanism due to the residual stresses. They assumed that some grain boundaries fracture on the first loading cycle, which relieves the residual stress in the adjacent grain, and then the misfit produced between grains can lead to the generation of tensile stresses on unloading by wedging, local contact stresses and shear, leading to fracture of additional grain boundaries. These mechanisms caused by the residual stresses appear to be possible in ceramic materials.

### 4.3 Asperities of crack surfaces

In ceramic materials asperities are easily produced on the crack surfaces, which might presumably be caused by the residual stresses described above, or friction and wear,[6] or a phase transformation. These asperities seem to be important because it is considered that they result in two types of damage effects:

(a) Indentation damage.[3] During unloading and/or compressive loading of stress cycling, extremely high stress arises at the asperity-contact on the crack surfaces, and consequently indentation damage develops there. This model, proposed by Evans,[3] is shown in Fig. 10. Local plastic deformation due to the compressive stress initiates lateral cracks during unloading so that the total crack length is increased.

(b) Wedge effect or particle trapping effect. In some ceramic materials small particles debond from the material without difficulty.

Trapping of these debonded particles inside the crack surfaces is also considered to be one of the reasons for the generation of asperity-contact. These asperities may give rise to another type of effect, which is schematically shown in Fig. 11. The particles trapped inside the crack during tensile loading increase the stress at the crack tip during subsequent unloading or compressive loading, as these ceramic particles are too hard to deform plastically. It is assumed that in metals and alloys this effect is insignificant, whereas in ceramic materials it may be important.

In $Si_3N_4$ materials crack propagation has been observed to occur intergranularly (Fig. 6), whereas in SiC materials, which do not reveal the cyclic effect, the fracture path is transgranular.[9] Such a tendency implies that cyclic damage in ceramic materials is

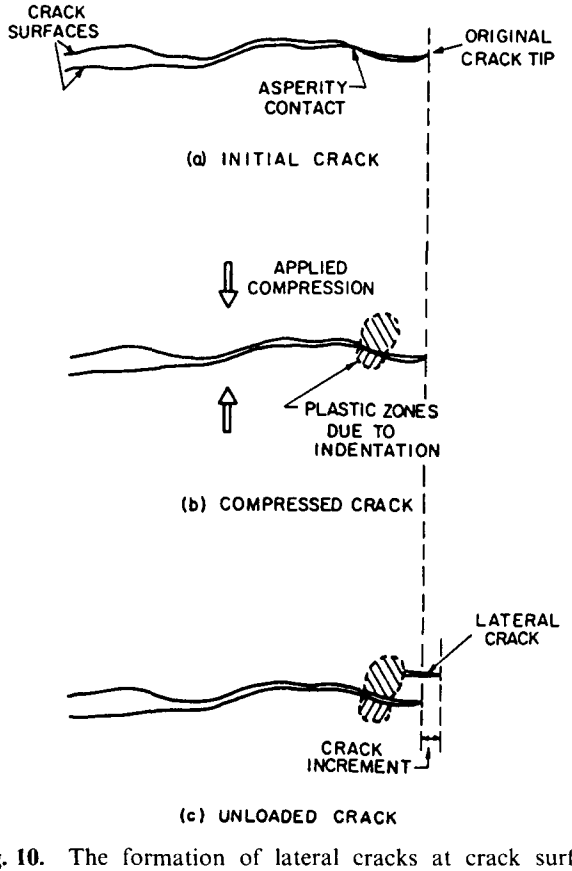


**Fig. 10.** The formation of lateral cracks at crack surface asperities (Evans[3]).

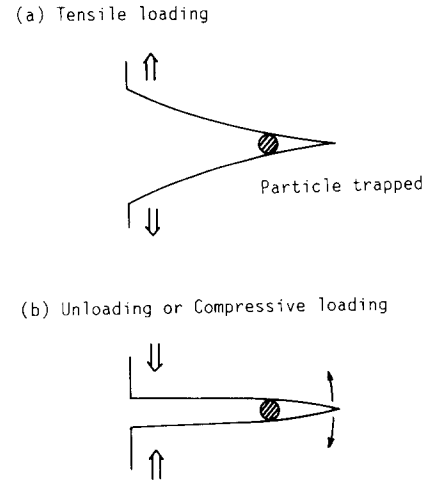


**Fig. 11.** The particles trapped inside the crack increase $K$ at the crack tip during subsequent unloading or compressive loading.

closely related to the asperity of the crack surface. In particular, observation of the morphology near the crack (see Fig. 8) suggests that the lateral cracking mechanism ((a) above) might be operative, although further experiments are required to demonstrate this conclusively. These mechanisms or models relevant to asperities are supported by the fact that during cyclic loading pre-existing cracks of the maximum size do not propagate, but instead a newly produced indentation crack grows (as described in Fig. 9).

## 5 Concluding Remarks

Cyclic fatigue properties of normally sintered and reaction-bonded silicon nitride materials were investigated and the validity of the fatigue mechanisms proposed up to now have been discussed. The main results obtained are as follows.

(1) In the silicon nitride ceramic materials used in the experiment the crack propagates by cyclic loading even under the condition of $K_{max} < K_{ISCC}$.

(2) It has been observed that a surface upheaval is produced in the region near the cyclically propagating cracks and, moreover, that a different type of crack is formed at the base of the hill.

(3) Although the precise fatigue mechanism for $Si_3N_4$ materials is still unclear, it is supposed that asperity-contacts of the crack surfaces are closely related to the fatigue damage behavior.

## Acknowledgements

The author gratefully acknowledges both the provision of analysing facilities and the help of Mr Y. Taguchi, Mr T. Wakamatsu and Mr R. Hirahara.

## References

1. Krohn, D. A. & Hasselman, D. P. H., Static and cyclic fatigue behavior of a polycrystalline alumina. *J. Am. Ceram. Soc.*, **55**(4) (1972) 208–11.
2. Evans, A. G., Microfracture from thermal expansion anisotropy—single phase systems. *Acta Metall.*, **26** (1978) 1845–53.
3. Evans, A. G., Fatigue in ceramics. *Int. J. Fracture*, **16** (1980) 485–98.
4. Lewis, D. & Rice, R. W., Comparison of static, cyclic, and thermal-shock fatigue in ceramic composites. *Ceram. Eng. Sci. Proc.*, **3** (1982) 714–21.
5. Lewis, D. III, Cyclic mechanical fatigue in ceramic–ceramic composites—an update. *Ceram. Eng. Sci. Proc.*, **4** (1983) 874–81.
6. Grathwohl, G., Ermüdung von Keramik unter Schwingbeanspruchung. *Mat.-wiss. Werkstofftech.*, **19** (1988) 113–24.
7. Heinrich, J. & Hausner, H., Microstructure and mechanical properties of reaction bonded silicon nitride. In *Energy and Ceramics, Proc. 4th Int. Meeting on Modern Ceram. Tech.*, ed. P. Vincenzini. Elsevier, Amsterdam, 1980, pp. 780–92.
8. Ziegler, G. & Heinrich, J., Microstructural changes during annealing of reaction-bonded $Si_3N_4$ and their influence on thermal diffusivity. In *Science of Ceramics*, Vol. 11. Swedish Ceramic Society, Göteborg, 1981, pp. 511–18.
9. Horibe, S. & Sumita, M., Fatigue behavior of sintered SiC; temperature dependence and effect of doping with aluminium. *J. Mater. Sci.*, **23** (1988) 3305–13.
10. Horibe, S., Cyclic fatigue crack growth from indentation flaw in $Si_3N_4$. *J. Mater. Sci. Lett.*, **7** (1988) 725–7.
11. Marshall, D. B. & Lawn, B. R., Flaw characteristics in dynamic fatigue: the influence of residual contact stresses. *J. Am. Ceram. Soc.*, **63**(9–10) (1980) 532–6.